Plant Cell Reports (2019) 38:147–159
https://doi.org/10.1007/s00299-018-2356-8

ORIGINAL ARTICLE

Expression of seven carbonic anhydrases in red alga *Gracilariopsis chorda* and their subcellular localization in a heterologous system, *Arabidopsis thaliana*

Md. Abdur Razzak[1] · JunMo Lee[2] · Dong Wook Lee[1] · Jeong Hee Kim[3,4] · Hwan Su Yoon[2] · Inhwan Hwang[1,5]

Received: 9 October 2018 / Accepted: 7 November 2018 / Published online: 16 November 2018

Abstract

Key message **Red alga, *Gracilariopsis chorda*, contains seven carbonic anhydrases that can be grouped into α-, β- and γ-classes.**

Abstract Carbonic anhydrases (CAHs) are metalloenzymes that catalyze the reversible hydration of CO_2. These enzymes are present in all living organisms and play roles in various cellular processes, including photosynthesis. In this study, we identified seven CAH genes (*GcCAHs*) from the genome sequence of the red alga *Gracilariopsis chorda* and characterized them at the molecular, cellular and biochemical levels. Based on sequence analysis, these seven isoforms were categorized into four α-class, one β-class, and two γ-class isoforms. RNA sequencing revealed that of the seven CAHs isoforms, six genes were expressed in *G. chorda* in light at room temperature. In silico analysis revealed that these seven isoforms localized to multiple subcellular locations such as the ER, mitochondria and cytosol. When expressed as green fluorescent protein fusions in protoplasts of *Arabidopsis thaliana* leaf cells, these seven isoforms showed multiple localization patterns. The four α-class GcCAHs with an N-terminal hydrophobic leader sequence localized to the ER and two of them were further targeted to the vacuole. GcCAHβ1 with no noticeable signal sequence localized to the cytosol. The two γ-class GcCAHs also localized to the cytosol, despite the presence of a predicted presequence. Based on these results, we propose that the red alga *G. chorda* also employs multiple CAH isoforms for various cellular processes such as photosynthesis.

Keywords Carbonic anhydrase · Subcellular localization · CO_2 · Phylogenetic tree · *Gracilariopsis chorda* · Red algae

Communicated by Youn-Il Park.

Electronic supplementary material The online version of this article (https://doi.org/10.1007/s00299-018-2356-8) contains supplementary material, which is available to authorized users.

✉ Inhwan Hwang
ihhwang@postech.ac.kr

[1] Division of Integrative Biosciences and Biotechnology, Pohang University of Science and Technology, Pohang 37673, South Korea

[2] Department of Biological Sciences, Sungkyunkwan University, Suwon 16419, South Korea

[3] Department of Biochemistry and Molecular Biology, College of Dentistry, Kyung Hee University, Seoul 130-701, South Korea

[4] Department of Life and Nanopharmaceutical Sciences, Graduate School, Kyung Hee University, Seoul 130-701, South Korea

[5] Department of Life Sciences, Pohang University of Science and Technology, Pohang 37673, South Korea

Introduction

Carbonic anhydrases (CAH, EC 4.2.2.1) are a family of enzymes that catalyze the interconversion of carbon dioxide and water into bicarbonate and a proton according to the following reaction:

$$CO_2 + H_2O \leftrightarrow HCO_3^- + H^+.$$

Since the active site of carbonic anhydrases contains a zinc ion, these proteins are also referred to as metalloenzymes (Coleman et al. 1967; Lindskog et al. 1997). Five distinct classes (α-, β-, γ-, δ-, and ξ-class) of carbonic anhydrases are found throughout nature (DiMario et al. 2018). The α-class CAHs are the most abundant and commonly found in vertebrates, bacteria, algae, and green plants, whereas β-class CAHs are found in bacteria, algae, and land plants. The γ-class CAHs are mainly found in land plants. The two remaining classes, the δ- and ξ-class, are less well studied and have been identified in marine diatoms to date

(Zimmerman et al. 2010; MacAuley et al. 2009; Ferry et al. 2010; DiMario et al. 2018). Although all CAHs have a common catalytic function, these five classes of CAHs differ significantly from each other in terms of amino acid sequence, structure, and activity due to their divergent evolutionary origins (DiMario et al. 2017). For instance, the α-class CAHs also have esterase activity (Jacob et al. 1967; Di Fiore et al. 2015).

Under the same enzymatic activity of the hydration of CO_2, the exact physiological roles of CAHs are dependent on the individual organism. For example, in bacteria, CAHs are involved in the production of many metabolites, including nucleotides and amino acids (Smith et al. 2000; Supuran et al. 2017). In humans, CAHs maintain the acid base balance or pH balance between blood and plasma or the release of CO_2 in the lung (Arthurs et al. 2008). In plants and algae, CAHs play a crucial role in photosynthesis. In algae, CAHs are involved in a specific mechanism, called CCM (CO_2-concentrating mechanism), which captures CO_2 in the cytosol and releases it into carboxysomes or pyranoids to facilitate photosynthesis (Atkinson et al. 2016; Gee et al. 2017). In plants, CAHs have recently gained increasing attention because of the possibility of using them to increase the photosynthetic efficiency of crop plants (Parisi et al. 2004; Wang et al. 2012). Because CAHs are one of the CCM components in algae and C4 plants, CAHs and bicarbonate transporters were introduced into C3 plants for the purpose of setting up the CCM mechanism (Atkinson et al. 2016). In addition, CAHs play an important role in amino acid production and in monitoring cellular CO_2 levels in plants (DiMario et al. 2017).

The physiological roles of CAHs are closely related to their subcellular localization. Therefore, information on the localization of CAHs is crucial for a full understanding of the physiological roles of multiple CAH isoforms in an organism. CAHs are found in various subcellular compartments. For example, in *Arabidopsis thaliana*, α-, β-, and γ-class CAHs are localized to the chloroplast, cytosol and mitochondria, respectively, where they play specific roles (Moroney et al. 2001; Fabre et al. 2007). The localization of multiple CAHs has been well characterized in *Chlamydomonas reinhardtii*: CAH1 and CAH2 to the periplasm, CAH3 to the thylakoid lumen, CAH4 and CAH5 to the mitochondria, CAH6 to the chloroplast stroma, CAH8 to the PM/periplasm, CAH9 to the cytoplasm, and the γ-class isoforms CAG1, CAG2, and CAG3 to mitochondria (Cardol et al. 2005; Fabre et al. 1996; Fujiwara et al. 1990; Karlsson et al. 1995; Mitra et al. 2004; Moroney et al. 2001, 2011; Ynalvez et al. 2008). In other organisms, CAHs are also found in other cellular organelles such as the ER and vacuole (Gee et al. 2017; DiMario et al. 2018). These CAHs show preferential localization patterns depending on their classes. Although there are a few exceptions, α-, β-, γ-class CAHs generally localize to the chloroplasts, cytosol, and mitochondria, respectively (DiMario et al. 2017).

In this study, we investigated *CAH* genes in the genome sequence of *Gracilariopsis chorda* to determine their expression and subcellular localization in a heterologous system, *Arabidopsis thaliana*. *G. chorda* is an economically important agar-producing multicellular marine red algal species (Rhodophyta, Florideophyceae). In an attempt to elucidate the biology of this organism, whole genome sequencing is currently underway (Lee et al. 2018a). Based on the draft genome data, we identified genes encoding CAHs in this study. Then we examined the expression of these genes in *G. chorda*. We also examined the subcellular localization of these genes in a heterologous system, *Arabidopsis thaliana*. We provided evidence that of the seven *GcCAHs*, six isoforms were well expressed in *G. chorda* in light at room temperature and that the seven GcCAH isoforms localized to various organelles such as the ER, vacuole, and cytosol in *Arabidopsis*.

Materials and methods

Phylogenetic analysis of *GcCAHs*

Homologs of the seven *GcCAHs* were collected by BLAST (e value $\leq e^{-05}$) analysis of the UniProt database (http://www.uniprot.org). These homologous genes were aligned using MAFFT 7.313 with default settings (Katoh and Toh 2008). Each alignment was used to infer phylogenetic relationships based on the maximum likelihood (ML) method using IQ-Tree v1.3.0 with the automatic model selection option (-m TEST). Branch support values were obtained with the ultrafast bootstrap method implemented in IQ-Tree, with 1000 replications (Minh et al. 2013; Flouri et al. 2015; Nguyen et al. 2015).

Identification and expression analysis of CAHs in *Gracilariopsis chorda*

G. chorda was collected from a coastal farm in Jangheung, Jeonnam, Korea (34°28′18" N 126°56′28" E) on 2 February, 2013. Seven *CAH* genes were identified by BLAST analysis of *G. chorda* genome data (Lee et al. 2018a) and domain searches (CD-search; Marchler-Bauer et al. 2016). Gene expression analysis was performed using RNA sequencing (RNA-seq) data generated from *G. chorda* under seven culture conditions (Lee et al. 2018a): (1) cleaned vegetative thallus [light (2 h) and room temperature (RT; 20 °C)]; (2) female thallus [light and RT]; (3) vegetative thallus [light and high temperature (30 °C, 2 h)]; (4) vegetative thallus [light and half salinity condition (DW: seawater = 1:1)]; (5) vegetative thallus [dark (2 h) and RT]; (6) vegetative

thallus [light (30 min) after dark treatment (7 h)]; (7) vegetative thallus [light and low temperature (4 °C, 7 days)]. The expression levels of *GcCAHs* were investigated using the 'Salmon' program (Patro et al. 2017) and represented as TPM (transcripts per million) values.

Prediction of organellar targeting signals

Subcellular localization of seven GcCAH isoforms was predicted by in silico analysis. TargetP (http://www.cbs.dtu.dk/services/TargetP/), PSORT (https://psort.hgc.jp/), and PREDOTAR (https://urgi.versailles.inra.fr/Tools/Predotar) were used to predict the subcellular localizations of the GcCAHs isoforms of *G. chorda*. SignalP was used to predict the leader sequence cleavage site (Emanuelsson et al. 2000). To corroborate these predictions, Protscale/ExPASy, a method specific for ER-targeted proteins, was used to analyze the hydrophobicity of GcCAHα1, GcCAHα2, GcCAHα3, and GcCAHα4.

Plant growth conditions

Arabidopsis thaliana (Columbia-0 ecotype) was grown in a growth chamber at 22–23 °C with a 16 h light/8 h dark cycle on Gamborg B5 agar plates. Leaf tissues were harvested from 2- to 3-week-old plants for protoplast preparation (Ahn et al. 2017).

Plasmid construction

The DNA fragments encoding seven GcCAHs isoforms were isolated by PCR with *GcCAH* isoform-specific forward and reverse primers using genomic DNA as template. The primer sequences are shown in Supplemental Table S2. The PCR products were ligated into the 326-sGFP vector containing sGFP (Kim et al. 2013). To fuse a small epitope HA (hemagglutinin) tag at the C-terminus of 4 α-class GcCAHs, PCR products were digested with Xba1 and BamH1 and ligated into HA-containing 326-vector (Lee et al. 2018b) which was also digested with Xba1 and BamH1.

PEG-mediated transformation of *Arabidopsis* protoplasts

Plasmid DNA was purified using a Qiagen MIDI kit (Qiagen). Plasmid DNA was transformed into *Arabidopsis* protoplasts via PEG-mediated transformation (Lee et al. 2011a, b). Briefly, leaf tissues from 2- to 3-week-old *Arabidopsis* plants were incubated in enzyme solution containing cellulase and macerozyme with gentle agitation for 24 h. The protoplast solution was passed through a 100 µm mesh to remove debris. Harvested protoplasts were loaded onto 21% sucrose solution, followed by centrifugation at 98×*g* for 10 min. Intact protoplasts were isolated from the top and interface, and used for PEG-mediated transformation using 10 µg plasmid DNA.

Subcellular localization of GcCAHs:sGFP fusion proteins in Arabidopsis protoplasts

Images of GFP fluorescence and red chlorophyll autofluorescence were acquired by fluorescence microscopy (Lee et al. 2011a, b; Park et al. 2016). Images were obtained using a cooled CCD camera and a Zeiss Axioplan fluorescence microscope at 40× magnification. The filter sets used were XF116 (excitation, 474AF20; dichroic, 500DRLP; emission, 510AF23) and XF137 (excitation, 540AF30; dichroic, 570DRLP; emission, 585ALP) (Omega, Inc. Brattleboro, VT) for GFP and chlorophyll autofluorescence, respectively.

Western blot analysis

To prepare total protein extracts, transformed protoplasts were re-suspended in extraction buffer (50 mM Tris–HCl, pH 7.5, 150 mM NaCl, 1 mM EDTA, 1% Triton X-100, and 1× protease inhibitor cocktail) and lysed by brief sonication. The cell lysates were centrifuged at 3000×*g* at 4 °C for 10 min to remove cellular debris. Protein extracts were separated by SDS/PAGE and subjected to western blot analysis. Mouse monoclonal anti-GFP antibody was used (at a dilution at 1:1000, Clontech, Cat. #632381) as primary antibody and anti-mouse IgG (at a dilution at 1:5000) was used as a secondary antibody. For HA-fused α-class GcCAHs, rat monoclonal anti-HA (Roche, Cat. #11867423001) antibody was used as a primary antibody and secondary anti-rat IgG was used to detect the primary antibody. Rabbit polyclonal anti-BiP antibody (Bioapp, Korea) was used to detect BiP. Protein bands were visualized using enhanced chemiluminescence (ECL kit; Amersham Pharmacia Biotech), and images were obtained using a LAS 4000 image capture system (Fujifilm, Japan).

TCA precipitation of secreted proteins

Proteins were prepared from protoplast incubation medium using TCA (trichloro acetic acid) (Koontz 2014). Briefly, a 0.1 volume of 100% TCA (100 µL) was added to the protoplast incubation medium after the precipitation of protoplasts and incubated at 4 °C for 60 min. The pellet fraction was collected after centrifugation at 14,000×*g* for 10 min and washed with ether:ethanol (1:1) solution. The pellet was collected after centrifugation at 14,000×*g* for 5 min and dried at room temperature. The dried pellet was dissolved in 0.1 N NaOH. Proteins were denatured using 6× loading buffer [30% (V/V) glycerol, 0.25% (W/V), 0.25% (W/V) xylene cyanol FF], followed by boiling for 5 min for SDS/

PAGE analysis. Mouse monoclonal GFP antibody was used (at a dilution at 1:1000, Clontech, Cat. #632381) for western blot analysis.

Mitochondrial staining by MitoTracker red

For mitochondria detection, transformed protoplasts were stained with 200 nM MitoTracker red (CM-H2XROS; Molecular Probes, Invitrogen). Prior to image capturing, the cells were incubated in the dark for 1 h. Images were captured under a fluorescence microscope with the FL-closed option using a cooled CCD camera and a Zeiss Axioplan fluorescence microscope at 40 × magnification.

Results

Phylogenetic analysis of *G. chorda* CAHs

We identified seven genes encoding CAHs (*GcCAHs*) from the genome sequence of *G. chorda* based on amino acid sequence homology by BLAST using UniProt (http://www.uniprot.org). These seven isoforms could be grouped into three classes, with four, one, and two isoforms belonging to the α-, β-, γ-classes, respectively (Table 1). To better understand the relationship of these seven isoforms, we performed phylogenetic analysis of these proteins, including homologs in other organisms. Four α-class isoforms, GRC0025GENE2732 (GcCAHα1), GRC0050GENE4227 (GcCAHα2), GRC0127GENE6767 (GcCAHα3), and GRC0173GENE7950 (GcCAHα4), showed a close relationship with land plants, with high bootstrap supports (83–96%) (Fig. 1a–d; Supplemental Figure S1A–D). One β-class isoform, GRC0011GENE1278 (GcCAHβ1), showed a high degree of homology to bacterial CAHs (i.e., *Mycobacterium tuberculosis*) that this isoform is regarded to be of bacterial origin (Fig. 1e; Supplemental Figure S1E). In addition, *G. chorda* contains a very limited number of β-class CAHs, which are usually present in the cytosol in other algae and land plants. The two other isoforms, GRC0109GENE6253 (GcCAHγ1) and GRC0223GENE8865 (GcCAHγ2), share a close relationship with the mitochondria-localized CAHs from *Arabidopsis* (Fig. 1f, g and Supplemental Figure S1F and S1G). These results indicate that these α- and γ-class CAH isoforms in *G. chorda* share common ancestors with those of land plants.

Table 1 Classification of *Gracilariopsis chorda* CAHs

Accession number	Category	Given name
GRC0025GENE2732	Alpha class	GcCAHα1
GRC0050GENE4227	Alpha class	GcCAHα2
GRC0127GENE6767	Alpha class	GcCAHα3
GRC0173GENE7950	Alpha class	GcCAHα4
GRC0011GENE1278	Beta class	GcCAHβ1
GRC0109GENE6253	Gamma class	GcCAHγ1
GRC0223GENE8865	Gamma class	GcCAHγ2

The classification of CAH of *G. chorda* was based on amino acid sequence homology to CAHs in other organisms. Homologs of seven GcCAH isoforms were collected by BLASTp using the UniProt database. These homologs were aligned and used to prepare phylogenetic trees. The GcCAHs were classified into three classes, α-, β-, and γ-classes, based on maximum homology

CAHs expression in *Gracilariopsis chorda*

To gain insight into the physiological roles of these CAHs in *G. chorda*, we examined the expression of *CAHs* based on RNA-seq data (Lee et al. 2018a) from *G. chorda* grown under seven different conditions, where the light, dark, and temperature were the parameters (details in "Materials and methods"). All *CAHs* except *GcCAHα4* were expressed in *G. chorda*, although their expression levels varied depending on the isoform; these *CAHs* showed the highest expression levels in the light at room temperature 20 °C (conditions 1 and 2) and reduced expression levels in the dark and at very high or very low temperatures (conditions 3, 5, 6, and 7) (Fig. 2; Supplemental Table S1a). These results indicate that light and temperature are crucial factors for the expression of *GcCAHs*. Moreover, the light-dependent expression of these genes suggests that they play a critical role in photosynthesis. In addition, depending on the growth conditions, these seven genes showed different expression patterns. We assessed the significance of the differences in the expression patterns depending on the growth conditions by statistical analysis. The Wilcoxon signed rank test using R statistical software was used for statistical analysis. We compared TPM (transcript per million) values of the seven GcCAHs genes between condition 1 (standard) and the others. This statistic test is suitable for the comparison of two groups with small sampling sizes (i.e., TPM values of 7 genes). For example, we compared seven TPM values of *CAH* genes between condition 1 and condition 3, but these two expression patterns did not show any significant difference (p value: 0.1094), although the seven genes showed different levels of TPM values. Similarly, under other conditions, there are no significant differences (p values > 0.05). In conclusion, there was no significant difference in the expression patterns of seven CAH genes between culture conditions (Supplemental Table S1b).

In silico analysis reveals multiple subcellular localizations of GcCAHs in the cell

The physiological roles of CAHs strongly depend on their subcellular localization (Morony et al. 2001, 2011). Thus,

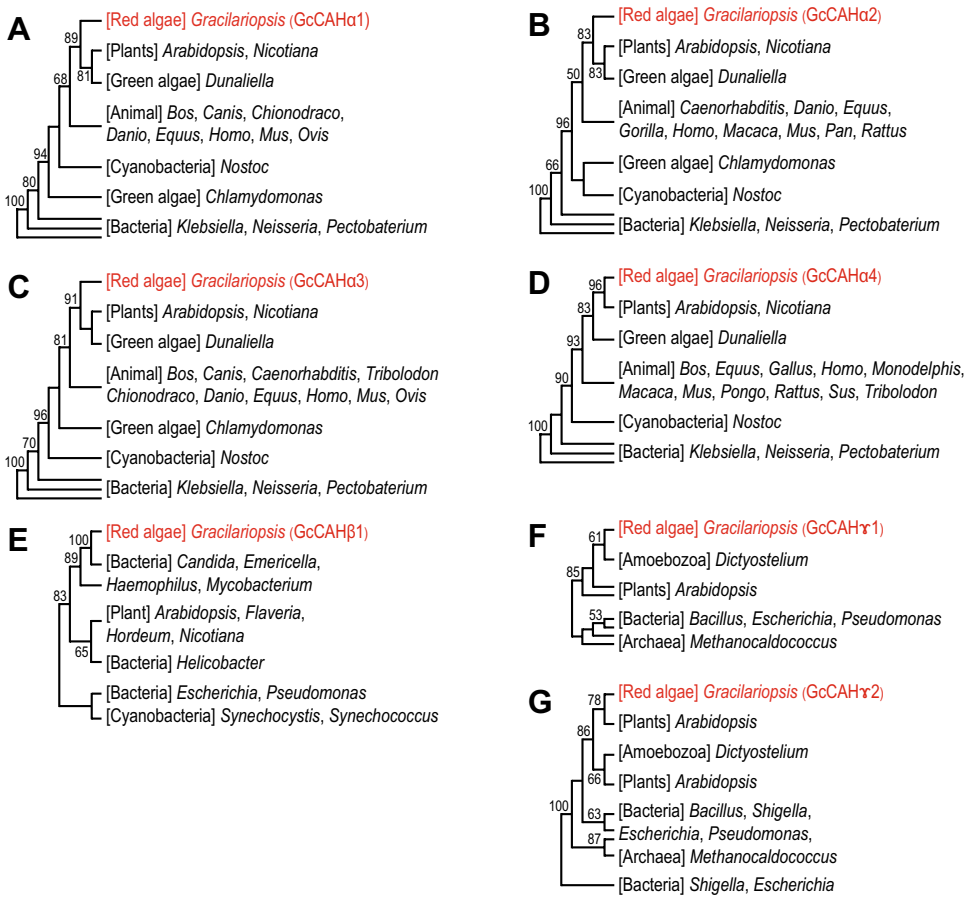

Fig. 1 Phylogenetic analysis of *GcCAHs* in *Gracilariopsis chorda*. **a–g** Phylogenetic trees for the seven *GcCAHs* were generated using the maximum likelihood (ML) method to investigate the maximum homology among several species. GcCAHs were classified based on homology among CAHs in different species. These GcCAHs were named according to classification based on amino acid homology

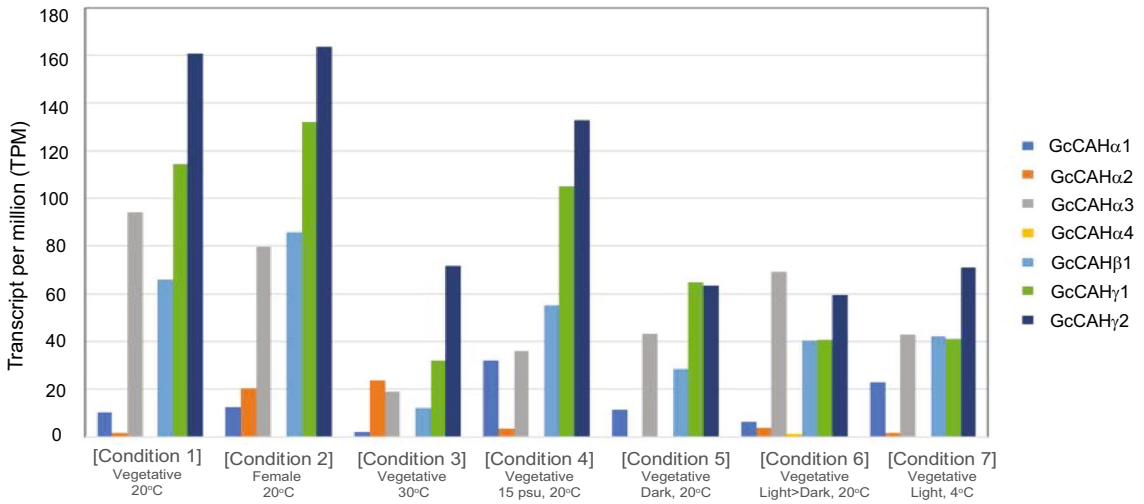

Fig. 2 The expression patterns of *GcCAHs* in *Gracilariopsis chorda*. mRNA was isolated from *G. chorda* cultured under seven different conditions as described in the "Materials and methods" section, and transcript levels were analyzed by RNA-sEq. The expression levels of the *GcCAHs* were determined using the 'Salmon' program (Patro et al. 2017) and are represented as TPM (transcripts per million) values

to broaden our understanding of the roles of CAHs in *G. chorda*, we examined their subcellular localizations. In green algae (i.e., *Chlamydomonas reinhardtii*), CAHs are found in many different subcellular regions, such as the chloroplast, mitochondria, cytosol, and apoplast (Morony et al. 2001, 2011; Fujiwara et al. 1990). We analyzed the putative

localizations of these proteins using prediction tools such as PSORT, PREDOTAR, TargetP, and ChloroP. These analyses indicated that GcCAHα1, GcCAHα2, GcCAHα3, and GcCAHα4 have an N-terminal extension with a high degree of hydrophobicity (Table 2; Supplemental Figure S2) (Lee et al. 2011a, b) that could serve as a leader sequence for ER targeting, whereas GcCAHγ1 and GcCAHγ2 were predicted to contain a presequence for targeting to mitochondria. By contrast, GcCAHβ1 was predicted to lack any known organellar targeting signals and was therefore thought to localize to the cytosol. These results suggest that GcCAHs have three different subcellular locations in *G. chorda*.

GcCAHs localize to the ER, vacuole, and cytosol in the heterologous system, protoplasts of *Arabidopsis*

We examined the subcellular localizations of CAHs in a heterologous system, *Arabidopsis*, because a method for transforming DNA constructs into *G. chorda* are not currently available. To examine the localization of GcCAHs, we generated C-terminal GFP fusion constructs and introduced them into protoplasts from *Arabidopsis* leaf tissues

Table 2 In silico prediction of the subcellular localizations of GcCAHs

Protein	Prediction tool	Predicted localization
GcCAHα1	PSORT	Extracellular/cell wall
	TargetP and ChloroP	SP
	PREDOTAR	ER
GcCAHα2	PSORT	Vacuole/cell wall
	TargetP and ChloroP	SP
	PREDOTAR	ER
GcCAHα3	PSORT	ER
	TargetP and ChloroP	SP
	PREDOTAR	ER
GcCAHα4	PSORT	Extracellular/cell wall/vacuole
	TargetP and ChloroP	SP
	PREDOTAR	ER
GcCAHβ1	PSORT	Cytoplasm
	TargetP and ChloroP	Cytoplasm
	PREDOTAR	Elsewhere
GcCAHɣ1	PSORT	Mitochondria
	TargetP and ChloroP	Mitochondria
	PREDOTAR	Mitochondria
GcCAHɣ2	PSORT	Mitochondria
	TargetP and ChloroP	Mitochondria
	PREDOTAR	Mitochondria

The subcellular localizations of GcCAHs were predicted using several prediction tools, including PSORT, TargetP, ChloroP, and PREDOTAR. The leader sequence and cleavage site were predicted by SignalP

(Kim et al. 2013; Lee et al. 2011a, b). First, we examined the expression of these fusion constructs in *Arabidopsis* protoplasts by western blot analysis using an anti-GFP antibody. All seven GFP-fused *GcCAH* constructs were readily expressed in the *Arabidopsis* protoplasts with the expected molecular weight (Fig. 3a). Next, we examined the in vivo localization of these fusion proteins by examining green fluorescent signals under a fluorescence microscope. Signals from the four α-class GcCAHs (GcCAHα1, GcCAHα2, GcCAHα3, and GcCAHα4) showed a network pattern, indicating that they localize to the ER (Fig. 3b). Of these four ER-localized proteins, GcCAHα2:sGFP and GcCAHα4:sGFP showed a vacuolar pattern at later time points, indicating that they slowly traffic to the vacuole from the ER (Fig. 3b).

To confirm the network pattern of GcCAHα1, GcCAHα2, GcCAHα3, and GcCAHα4, we co-transformed these constructs into *Arabidopsis* protoplasts together with an ER marker construct, *BiP:mCherry*, and examined their localization patterns. These four GcCAHαs showed a high degree of co-localization with BiP:mCherry (Fig. 3c), confirming their ER localization. These results are consistent with those of bioinformatics prediction, as they have a hydrophobic leader sequence at the N-termini.

ER-targeted proteins can be secreted out of the cell to the apoplast (Sohn et al. 2003). Indeed, many CAHs are known to be secreted into the periplasmic region or the apoplast in algae and plants (Morony et al. 2001, 2011; Fujiwara et al. 1990). To test this idea, we prepared protein extracts from protoplast incubation medium and analyzed them by western blotting using an anti-GFP antibody. A negligible amount of protein was detected in the protoplast incubation medium only for GcCAHα3 and GcCAHβ1 (Fig. 3d). However, we failed to detect BiP, an ER protein, in the medium, confirming that cellular proteins did not leak during protein preparation. We included Sec-GFP as a positive secretory protein control (Liu et al. 2000). As reported previously, most Sec-GFP was detected in the incubation medium, indicating that Sec-GFP had been efficiently secreted from the protoplasts. Together, these results suggest that the ER-localized GcCAH proteins are ER-resident proteins in Arabidopsis.

Next, we examined the localization of GcCAHβ1, a β-class isoform. In contrast to the α-class GcCAHs, GcCAHβ1 showed a diffuse cytosolic localization pattern (Fig. 4), indicating that it localizes to the cytosol. Indeed, in silico analysis predicted that it does not contain any targeting signal. Similarly, many β-class CAHs in algae and plants localize to the cytosol (Hiltonen et al. 1998; DiMario et al. 2016, 2017).

Finally, we examined the localization patterns of the two γ-class GcCAHs. Both GcCAHγ1:sGFP and GcCAHγ2:sGFP also showed a diffuse cytosolic localization pattern, along with a few punctate structures. However,

the punctate stains did not overlap with MitoTracker red-stained mitochondria, indicating that these proteins are not imported into mitochondria (Fig. 5). These results are in contrast to the data from in silico analysis, which predicted the presence of presequences in GcCAHγ1 and GcCAHγ2 (Table 2). These results suggest that the presequences in GcCAHγ1 and GcCAHγ2 are not recognized by the mitochondrial import machinery in plants.

GcCAHα2:sGFP and GcCAHα4:sGFP are targeted to the vacuole via the Golgi apparatus

Of these four ER-localized proteins, GcCAHα2:sGFP and GcCAHα4:sGFP showed a vacuolar pattern at a later time point, indicating that they slowly traffic to the vacuole from the ER (Fig. 3b). In general, vacuolar proteins are initially targeted to the ER prior to their trafficking to the vacuole (Sohn et al. 2003; Hwang 2008; De Marchis et al. 2013; Xiang et al. 2013). Next, we examined the trafficking pathway of GcCAHα2:sGFP and GcCAHα4:sGFP to the vacuole. In *Arabidopsis*, proteins can traffic to the vacuole via Golgi-dependent or Golgi-independent routes (Park et al. 2016; De Marchis et al. 2013; Xiang et al. 2013). We co-transformed *GcCAHα2:sGFP* or *GcCAHα4:sGFP* into *Arabidopsis* protoplasts together with *Sar1[H74L]*, encoding a dominant negative mutant of Sar1 (Takeuchi et al. 2000), and examined their localization patterns. Sar1 is a crucial factor for COPII vesicle formation at the ER for trafficking to the Golgi, and a dominant negative mutant of *Sar1[H74L]* blocks trafficking at the ER. These two GcCAHs:sGFP showed an ER network pattern in the presence of *Sar1[H74L]* (Fig. 6), indicating that their trafficking to the vacuole was inhibited. These results suggest that GcCAHα2 and GcCAHα4 are transported from the ER to the vacuole in a Golgi-dependent manner.

ER-localized GcCAHα1, GcCAHα2, GcCAHα3, and GcCAHα4 are N-glycosylated

Proteins targeted to the ER for subsequent localization to endomembrane compartments or for secretion are often modified by N-glycosylation (Park et al. 2016; Aebi et al. 2013). Indeed, amino acid sequence analysis showed that these four α-class GcCAHs possess several putative N-glycosylation sites, which are represented as NXS/T (N, asparagin; X, any amino acid residues except proline; S, serine; and T, threonine) (Supplemental Figure S3). Moreover, *Arabidopsis* CAH1 is known to be glycosylated, and N-glycosylation is critical for its enzymatic activity (Burén et al. 2011). We examined whether these four proteins are N-glycosylated. When a protein is glycosylated, the N-glycosylated form shows a slightly higher molecular mass than the non-glycosylated form in SDS/PAGE (Wyszynski et al. 2010; Kang et al. 2018). We tagged four CAHs with the small epitope tag, HA, at their C-termini and transformed the resulting constructs into protoplasts. We treated protoplasts with or without tunicamycin, an inhibitor of N-glycosylation (Park et al. 2016; Wyszynski et al. 2010) after transformation, prepared total protein extracts from protoplasts, and analyzed them by western blotting using anti-HA antibody. All four CAHs showed a slight decrease in molecular mass when the protoplasts were treated with tunicamycin (Fig. 7), indicating that all of these proteins are N-glycosylated in *Arabidopsis* protoplasts.

Discussion

In this study, we provide evidence that agar producing the red alga *G. chorda* contains seven *CAH* genes including four α-class, one β-class and two γ-class isoforms. Phylogenetic analysis revealed different evolutionary paths: the GcCAHαs and GcCAHγs share the common ancestors with land plants whereas the single GcCAHβ1 shares common ancestor with bacterial CAHs in *Mycobacterium tuberculosis*. Moreover, the β-class has only one copy in *G. chorda*, which is much lower than the number in plants and other algae (Fig. 1a–e; Supplemental Figure S1A–E). *Chlamydomonas reinhardtii* has two β isoforms CAH7 and CAH8 (Ynalvez et al. 2008). It is not clear whether this difference is related to the physiological difference between the multicellular red alga *G. chorda* and the single-celled green alga *C. reinhardtii*. In fact, overall, *G. chorda* appears to have fewer CAH isoforms than green algae and land plants.

Gracilariopsis chorda is a red alga with a maximum growth during spring to early summer (15–20 °C) in normal seawater salinity (ca. 34 practical salinity unit). RNA-seq analysis revealed that all *GcCAHs* except *GcCAHα4* were expressed at high levels in *G. chorda* in light, but at low levels in the dark (Fig. 2). The light-dependent expression of these genes raises the possibility that they are involved in photosynthesis, as in other organisms (Dionisio et al. 1990; Harada et al. 2005). Temperature was also a critical factor for their expression; these genes were expressed at high levels at room temperature (20 °C), but at low levels at high (30 °C) and low (4 °C) temperature condition. As *G. chorda* is a red alga that thrives in seawater, the *GcCAH* genes were highly expressed under salinity conditions (condition 4, Fig. 2). Overall, the expression patterns of *GcCAHs* varied depending on growth conditions, with growth in the light at room temperature being the most favorable condition.

The biochemical reaction carried out by CAHs is common to all CAHs. However, the physiological role of a particular isoform in a particular organism strongly depends on its subcellular localization. In silico analysis of these GcCAHs suggested that they might localize to

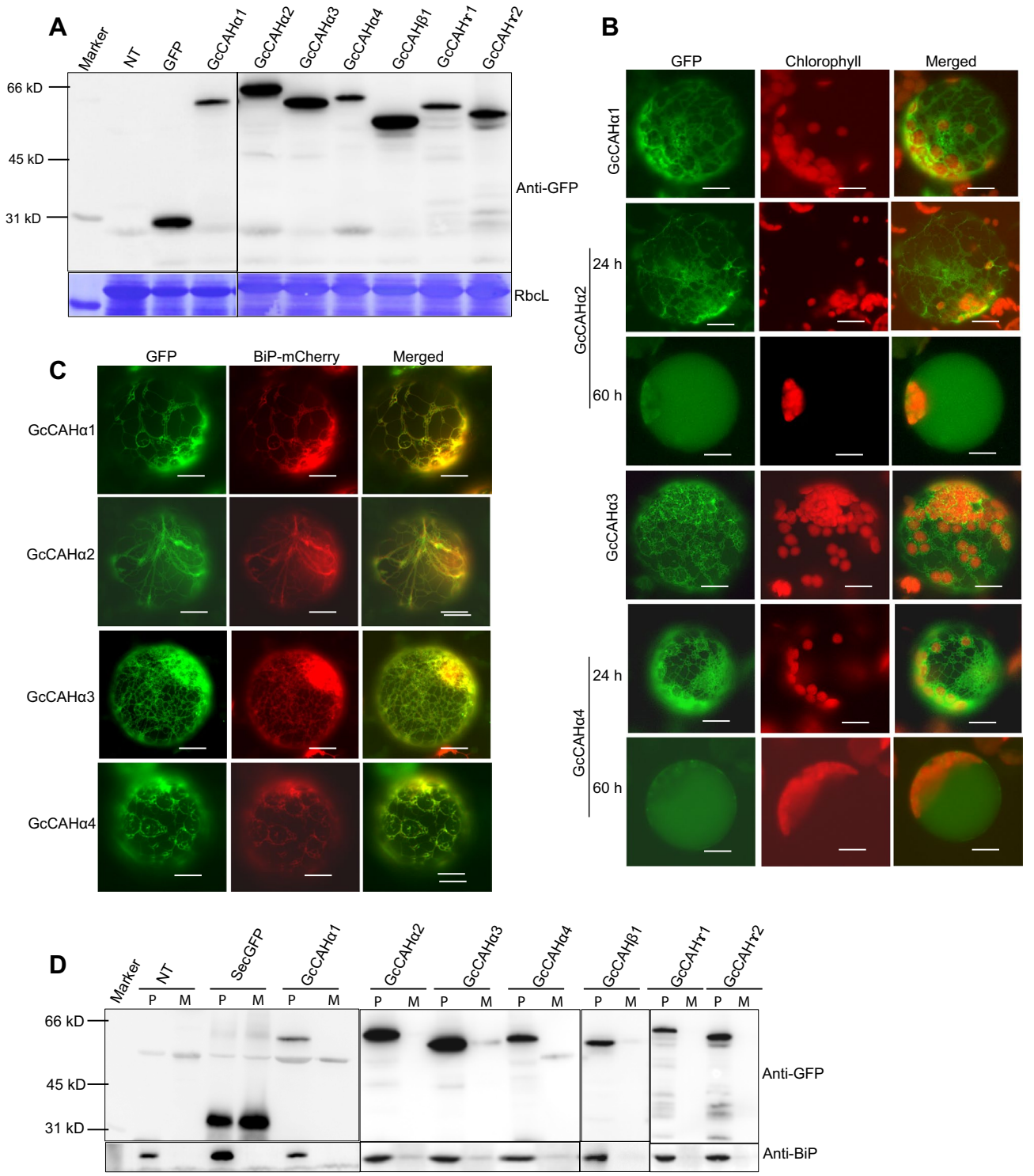

endomembrane compartments, mitochondria, and cytosol. This finding is consistent with earlier studies showing that multiple isoforms of CAHs are expressed and localize to many different subcellular organelles in algae such as *C. reinhardtii* (Morony et al. 2001, 2011; Fujiwara et al. 1990; Karlsson et al. 1995; Eriksson et al. 1996; Mitra et al. 2004; Ynalvez et al. 2008; Cardol et al. 2005).

To corroborate this finding, we used a heterologous system (*Arabidopsis* protoplasts) to examine the subcellular localization of these proteins in vivo. Of course, the use of heterologous systems may provide only a limited information on the exact locations of these proteins in *G. chorda*. Examining the subcellular localizations of GcCAHs in *Arabidopsis* protoplasts provided mixed results compared

◂**Fig. 3** Subcellular localization of sGFP-tagged GcCAHs in *Arabidopsis* protoplasts. **a** Western blot analysis of GcCAHs:sGFP. Arabidopsis protoplasts were transformed with the indicated constructs, and total protein extracts from transformed protoplasts were analyzed by western blotting with anti-GFP antibody. GFP alone was used as a positive control. RbcL (Rubisco large subunit) stained with Coomassie blue was used as a loading control. NT, non-transformed protoplasts used as a negative control. **b** In vivo localization of GcCAHs:sGFP. GFP patterns in protoplasts observed at 24 and 60 h after transformation. Green, red, and yellow signals represent GFP, chlorophyll autofluorescence, and the overlap between green and red signals, respectively. Scale bar 20 µm. **c** GcCAHα1:sGFP, GcCAHα2:sGFP, GcCAHα3:sGFP, and GcCAHα4:sGFP colocalize with BiP:mCherry. GcCAHα1:sGFP, GcCAHα2:sGFP, GcCAHα3:sGFP, and GcCAHα4:sGFP were co-transformed into protoplasts together with BiP:mCherry, an ER marker, and their colocalization was examined under a fluorescence microscope at 24 h after transformation. Green, red, and yellow signals represent GFP, BiP:mCherry, and the overlap between green and red signals, respectively. Scale bar = 20 µm. **d** Western blot analysis of GcCAHs expressed in Arabidopsis protoplasts. Protoplasts transformed with the indicated constructs were pelleted by centrifugation at 24 h after transformation and used for protein preparation. To prepare proteins in the protoplast incubation medium, the incubation medium was treated with trichloroacetic acid to precipitate the proteins. Secretory GFP (Sec-GFP) was used as a positive control for secretory proteins. Proteins from protoplasts and incubation medium were analyzed by western blotting with anti-GFP and anti-BiP antibodies. BiP was used as a control for ER proteins. For western blot analysis, 200 ng (10% of total proteins from protoplasts) and 200 ng (50% of proteins from the incubation medium) were loaded. NT, non-transformed protoplasts was used as a negative control. P, total proteins from protoplasts; M, proteins from the incubation medium. (Color figure online)

with the results of in silico analysis. The localization of GcCAHs predicted to be targeted to the ER was confirmed in *Arabidopsis* protoplasts. However, the prediction tool has limited ability to further define the exact locations of these proteins among various endomembrane compartments. In *Arabidopsis* protoplasts, of the four ER-targeted α-class GcCAHs, two isoforms, GcCAHα2 and GcCAHα4, further trafficked to the vacuole, albeit slowly (Fig. 3b), indicating that they behave as vacuolar proteins in *Arabidopsis*. This notion was confirmed by the fact that co-expression of a Sar1 dominant negative mutant, *Sar1 [H74L]*, blocked the ER-to-Golgi trafficking of these proteins (Takeuchi et al. 2000). In fact, vacuole-localized CAH has been identified in plants with CAM-type photosynthesis (DiMario et al. 2017). By contrast, the other two isoforms, GcCAHα1 and GcCAHα3, were present only at the ER. Consistent with this finding, all four ER-targeted proteins were post-translationally modified by N-glycosylation.

ER-localized CAHs and their function have been reported in other organisms. For example; in microalgae *Nannochloropsis oceanica*, ER-localized CAH1 (α class) is an essential component of CCM for photosynthesis (Gee et al. 2017; DiMario et al. 2018). Bicarbonate transporters pump bicarbonate (HCO_3^-) into the cytoplasm and then into the lumen of the ER, where carbonic anhydrase CAH1 also accumulates. CAH1 catalyzes from HCO_3^- formation of CO_2 which diffuses into the chloroplast stroma to be fixed by Rubisco (Gee et al. 2017). In a similar way, perhaps the ER-localized proteins, GcCAHα1 and GcCAHα3, might be involved in photosynthesis in *G. chorda*. However, we cannot exclude the possibility that these CAHs are initially targeted to the ER en route to other organelles such as the apoplast in *G. chorda*, but failed to be further targeted to their final locations in *Arabidopsis* due to the differences in sorting signals between red algae and *Arabidopsis*. Apoplastic proteins are transported through the endomembrane compartments after cotranslational targeting to the ER (Jin et al. 2001; Kim et al. 2013). In fact, CAH1 and CAH2 in *Chlamydomonas* localize to the apoplast (Morony et al. 2001, 2011; Fujiwara et al. 1990). Trafficking in the endomembrane compartments requires specific sorting or exit signals that cause the protein to exit the ER (Jin et al. 2001; Kim et al. 2013), and the exit signals of GcCAHαs might not be recognized by the trafficking machinery in *Arabidopsis*.

Another possible destination of ER-targeted GcCAHαs is the chloropast. Chloropast-localized AtCAHα1 in *Arabidopsis* is initially targeted to the ER and then transported to chloroplasts via the Golgi apparatus (Villarejo et al. 2005; Faye et al. 2006). Indeed, AtCAHα1 is modified by N-glycosylation, a hallmark of the ER, and the N-glycan is of the complex type, confirming its passage through the Golgi apparatus (Villarejo et al. 2005; Moroney et al. 2011). Thus, it is possible that some isoforms of these ER-targeted proteins may be targeted to chloroplasts in *G. chorda*. In support of this idea, none of the seven CAH isoforms showed any transit peptide or were targeted to chloroplasts in *Arabidopsis* protoplasts. However, it is well known that photosynthetic organisms contain multiple CAH isoforms in chloroplasts. Thus, the absence of transit peptide-containing CAHs in *G. chorda* strongly suggests that these CAHs might be transported to chloroplasts via a transit peptide-independent pathway, as observed in *Arabidopsis* (Villarejo et al. 2005). Thus, it is possible that some of these ER-targeted GcCAHαs is not faithfully targeted to chloroplasts in *Arabidopsis* (a heterologous system) due to the difference in the mechanisms of trafficking from the endomembrane compartments to chloroplasts between red algae and *Arabidopsis*. It is currently not fully understood how AtCAHα1 is transported from the Golgi to chloroplasts in *Arabidopsis*.

Another group of GcCAHs consisting of GcCAHγ1and GcCAHγ2 was predicted to contain a presequence for mitochondrial targeting. Consistent with this prediction, most γ-class CAHs are tageted to mitochondria (Ferry et al. 2010; Alber et al. 1994). However, in contrast to the prediction, these proteins were not targeted to mitochondria in *Arabidopsis* protoplasts, but instead produced a cytosolic pattern along with a few punctate stains. It is possible the plant machinery may not recognize the presequences of *G.*

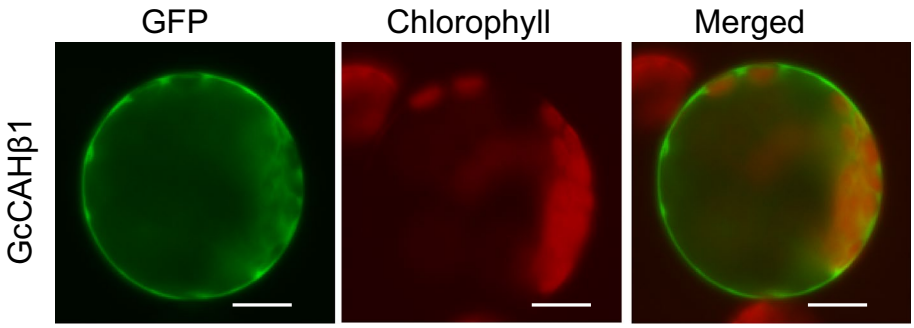

Fig. 4 Cellular localization of GcCAH beta isoform in *Arabidopsis* protoplasts. Localization of GcCAHβ1:sGFP. Protoplasts were transformed with *GcCAHβ1:sGFP*, and protein localization was examined under fluorescence microscope at 24 h after transformation. Scale bar 20 µm

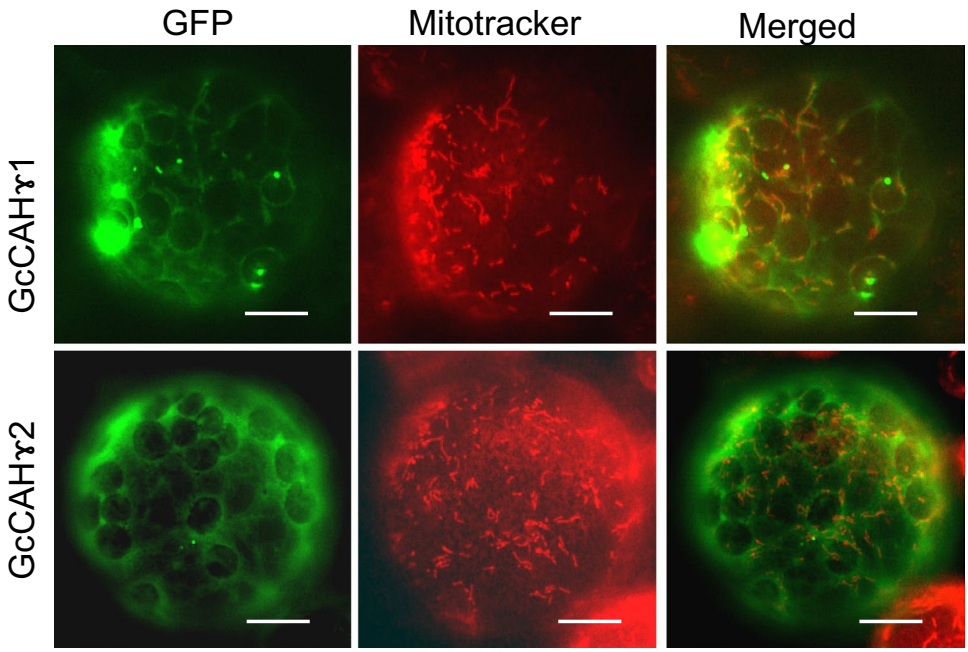

Fig. 5 Localization of sGFP-tagged GcCAH gamma isoforms in *Arabidopsis* protoplasts. Localization of GcCAHγ1:sGFP and GcCAHγ2:sGFP. Protoplasts were transformed with the indicated constructs. At 24 h aftertransformation, the protoplasts were stained with MitoTracker red and incubated for an additional 1 h, and the localization of theproteins was examined. Scale bar 20 µm

chorda. Indeed, the transit peptide of RbcS from *C. reinhardtii* failed to support protein import into chloroplasts in *Arabidopsis* (Razzak et al. 2017). Similarly, the presequence of GcCAHγ1 and GcCAHγ2 might not support protien import into mitochondria in *Arabidopsis* due to the difference in sequence motifs in the presequences.

The most important question about GcCAHs is their physiological roles in *G. chorda*. CAHs play a crucial role in photosynthesis in algae and plants. In fact, seawater contains relatively low levels of CO_2, and organisms living in seawater rely on the CCM for efficient photosynthesis (Gee et al. 2017; DiMario et al. 2018). Thus, in *G. chorda*, these CAHs might be involved in the CCM by converting CO_2 to HCO_3^-. CO_2 can easily pass through the lipid membranes, whereas HCO_3^- generally cannot. Thus, GcCAHs can help retain CO_2 in the cell in the form of HCO_3^-. Another important role of CAHs is to release CO_2 from HCO_3^- via the dehydration reaction. The Rubisco complex can use only CO_2 (Fujiwara et al. 1996). Thus, certain GcCAH isoforms may participate in photosynthesis in *G. chorda* via the dehydration reaction. Consistent with this idea, these genes showed strong light-dependent expression patterns. However, we currently cannot pinpoint which GcCAH isoforms are involved in the dehydration reaction of HCO_3^- to provide CO_2 to the Rubisco complex during photosynthesis. In addition to their role in photosynthesis, CAHs are also important for balancing cellular pH levels and amino acid biosynthesis (DiMario et al. 2017). Further studies are needed to elucidate the physiological roles of these GcCAHs in vivo.

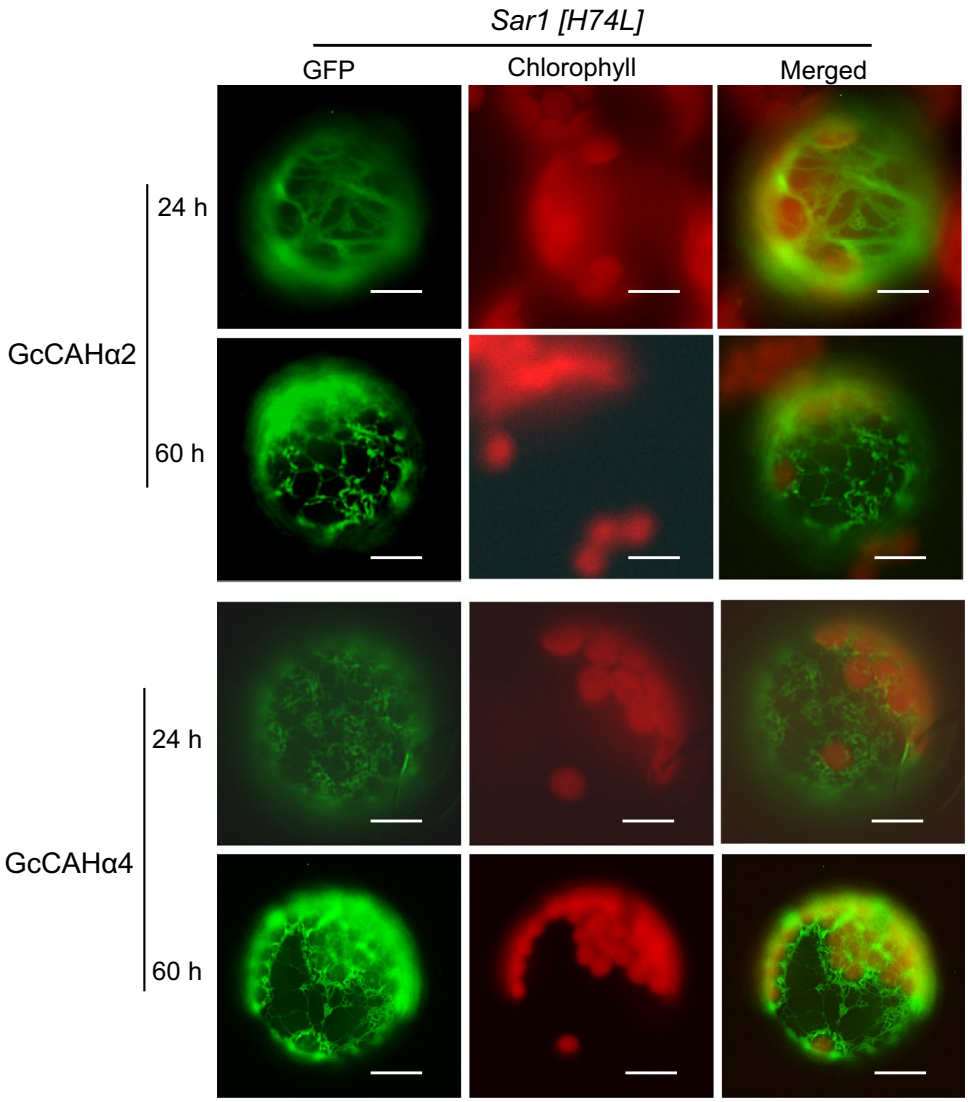

Fig. 6 Sar1[H74L] inhibits vacuolar trafficking of GcCAHα2 and GcCAHα4 at the ER. *GcCAHα2:sGFP* or *GcCAHα4:sGFP* was co-transformed into protoplasts together with *Sar1[H74L]*, and their localization was examined. Protoplasts were observed at 24 h and 60 h after transformation. Scale bar = 20 μm

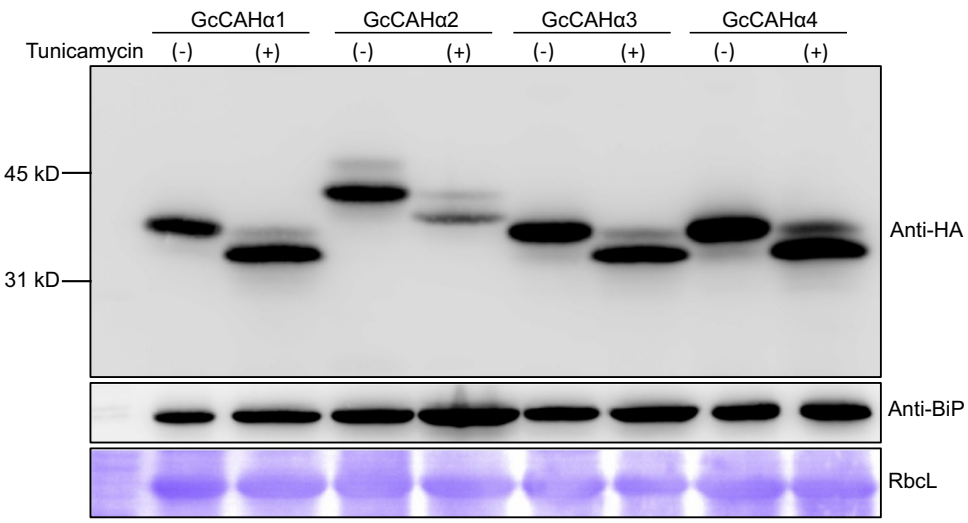

Fig. 7 ER-localized GcCAHα1, GcCAHα2, GcCAHα3, and GcCAHα4 are N-glycosylated. Protoplasts transformed with *GcCAHα1:HA, GcCAHα2:HA, GcCAHα3:HA*, or *GcCAHα4:HA* were incubated in the presence (+) or absence (−) of tunicamycin (10 μg/mL) for 24 h. Protein extracts were analyzed by western blottingusing anti-HA and anti-BiP antibodies. BiP and RbcL were used as loading controls

Author contribution statement MAR, JHK, and IH conceived the project. MAR performed most of the experiments. DWL performed in vivo imaging together with MAR. JL and HSY performed RNA-seq and phylogenetic analysis. MAR, HSY, and IH wrote the manuscript.

Acknowledgements This work was supported by grants from the National Research Foundation of Korea, Ministry of Science and ICT (No. 2016R1E1A1A02922014), and from the Collaborative Genome Program of the Korea Institute of Marine Science and Technology Promotion (KIMST) funded by the Ministry of Oceans and Fisheries (MOF) (20180430). Dong Wook Lee was supported by a grant from the Next-Generation BioGreen 21 Program (SSAC, grant number: PJ01335801), Rural Development Administration, Republic of Korea.

Compliance with ethical standards

Conflict of interest The authors declare no conflict of interest.

References

Aebi M (2013) N-linked protein glycosylation in the ER. Biochi Biophys Acta Mol Cell Res 1833:2430–2437. https://doi.org/10.1016/j.bbamcr.2013.04.001

Ahn G, Kim H, Kim DH et al (2017) SH3P2 plays a crucial role at the step of membrane tubulation during cell plate formation in plants. Plant Cell. https://doi.org/10.1105/tpc.17.00108

Alber BE, Ferry JG (1994) A carbonic anhydrase from the archaeon *Methanosarcina thermophila*. Proc Natl Acad Sci USA 91:6909–6913. https://doi.org/10.1073/pnas.91.15.6909

Arthurs GJ, Sudhakar M (2008) Carbon dioxide transport. Updat Anaesth 24:26–29. https://doi.org/10.1093/bjaceaccp/mki050

Atkinson N, Feike D, Mackinder LM et al (2016) Introducing an algal carbon-concentrating mechanism into higher plants: Location and incorporation of key components. Plant Biotechnol J 14:1302–1315. https://doi.org/10.1111/pbi.12497

Burén S, Ortega-Villasante C, Blanco-Rivero A et al (2011) Importance of post-translational modifications for functionality of a chloroplast-localized carbonic anhydrase (CAH1) in *Arabidopsis thaliana*. PLoS One. https://doi.org/10.1371/journal.pone.0021021

Cardol P (2005) The mitochondrial oxidative phosphorylation proteome of *Chlamydomonas reinhardtii* deduced from the genome sequencing project. Plant Physiol 137:447–459. https://doi.org/10.1104/pp.104.054148

Coleman JE (1967) Mechanism of action of carbonic anhydrase. J Biochem 242:5212–5219

De Marchis F, Bellucci M, Pompa A (2013) Unconventional pathways of secretory plant proteins from the endoplasmic reticulum to the vacuole bypassing the Golgi complex. Plant Signal Behav 8:1–5. https://doi.org/10.4161/psb.25129

Di Fiore A, Alterio V, Monti SM et al (2015) Thermostable carbonic anhydrases in biotechnological applications. Int J Mol Sci 16:15456–15480. https://doi.org/10.3390/ijms160715456

DiMario RJ, Quebedeaux JC, Longstreth DJ et al (2016) The cytoplasmic carbonic anhydrases β CA2 and β CA4 are required for optimal plant growth at low CO_2. Plant Physiol 171:280–293. https://doi.org/10.1104/pp.15.01990

DiMario RJ, Clayton H, Mukherjee A et al (2017) Plant carbonic anhydrases: structures, locations, evolution, and physiological roles. Mol Plant 10:30–46. https://doi.org/10.1016/j.molp.2016.09.001

DiMario RJ, Machingura MC, Waldrop GL, Moroney JV (2018) The many types of carbonic anhydrases in photosynthetic organisms. Plant Sci 268:11–17. https://doi.org/10.1016/j.plantsci.2017.12.002

Dionisio-Sese ML, Fukuzawa H, Miyachi S (1990) Light-induced carbonic anhydrase expression in *Chlamydomonas reinhardtii*. Plant Physiol 94:1103–1110. https://doi.org/10.1104/pp.94.3.1103

Eriksson M, Karlsson J, Ramazanov Z et al (1996) Discovery of an algal mitochondrial carbonic anhydrase: molecular cloning and characterization of a low-CO_2-induced polypeptide in *Chlamydomonas reinhardtii*. Proc Natl Acad Sci USA 93:12031–12034. https://doi.org/10.1073/pnas.93.21.12031

Fabre N, Reiter IM, Becuwe-Linka N, Genty B, Rumeau D (2007) Characterization and expression analysis of genes encoding alpha and beta carbonic anhydrases in *Arabidopsis*. Plant Cell Environ 30:617–629. https://doi.org/10.1111/j.1365-3040.2007.01651.x

Faye L, Daniell H (2006) Novel pathways for glycoprotein import into chloroplasts. Plant Biotechnol J 4:275–279. https://doi.org/10.1111/j.1467-7652.2006.00188.x

Ferry JG (2010) The γ class of carbonic anhydrases. Biochim Biophys Acta 1804:374–381. https://doi.org/10.1016/j.bbapap.2009.08.026

Flouri T, Izquierdo-Carrasco F, Darriba D et al (2015) The phylogenetic likelihood library. Syst Biol 64:356–362. https://doi.org/10.1093/sysbio/syu084

Fujiwara S, Fukuzawa H, Tachiki A, Miyachi S (1990) Structure and differential expression of two genes encoding carbonic anhydrase in *Chlamydomonas reinhardtii*. Proc Natl Acad Sci USA 87:9779–9783

Fujiwara S, Ishida N, Tsuzuki M (1996) Circadian expression of the carbonic anhydrase gene, Cah1, in *Chlamydomonas reinhardtii*. Plant Mol Biol 32:745–749. https://doi.org/10.1007/BF00020215

Gee CW, Niyogi KK (2017) The carbonic anhydrase CAH1 is an essential component of the carbon-concentrating mechanism in *Nannochloropsis oceanica*. Proc Natl Acad Sci U S A 114:4537–4542. https://doi.org/10.1073/pnas.1700139114

Harada H, Nakatsuma D, Ishida M, Matsuda Y (2005) Regulation of the expression of intracellular b-carbonic anhydrase in response to CO_2 and light in the marine diatom *Phaeodactylum tricornutum*. Plant Physiol 139:1041–1050. https://doi.org/10.1104/pp.105.065185.2004

Hiltonen T, Björkbacka H, Forsman C et al (1998) Intracellular beta-carbonic anhydrase of the unicellular green alga Coccomyxa. Cloning of the cDNA and characterization of the functional enzyme overexpressed in *Escherichia coli*. Plant Physiol 117:1341–1349. https://doi.org/10.1104/pp.117.4.1341

Hwang I (2008) Sorting and anterograde trafficking at the Golgi apparatus. Plant Physiol 148:673–683. https://doi.org/10.1104/pp.108.124925

Jacob A, Verpoorte, Mehta S, John T (1967) Esterase activities of human carbonic anhydrases B and C. J Biol Chem 242:4221–4229

Jin JB, Kim YA, Kim SJ et al (2001) A new dynamin-like protein, ADL6, is involved in trafficking from the trans-golgi network to the central vacuole in *Arabidopsis*. Plant Cell 13:1511–1526. https://doi.org/10.1105/tpc.13.7.1511

Kang H, Park Y, Lee Y, Yoo YJ, Hwang I (2018) Fusion of a highly N-glycosylated polypeptide increases the expression of ER-localized proteins in plants. Sci Rep 8:4612. https://doi.org/10.1038/s41598-018-22860-2

Karlsson J, Hiltonen T, Husic HD et al (1995) Intracellular carbonic anhydrase of *Chlamydomonas reinhardtii*. Plant Physiol 109:533–539. https://doi.org/10.1104/pp.109.2.533

Katoh K, Toh H (2008) Recent developments in the MAFFT multiple sequence alignment program. Brief Bioinform 9:286–298. https://doi.org/10.1093/bib/bbn013

Kim DH, Hwang I (2013) Direct targeting of proteins from the cytosol to organelles: the ER versus endosymbiotic organelles. Traffic 14:613–621. https://doi.org/10.1111/tra.12043

Koontz L (2014) TCA precipitation. Methods Enzymol 541:3–10. https://doi.org/10.1016/B978-0-12-420119-4.00001-X

Lee DW, Hwang I (2011) Transient expression and analysis of chloroplast proteins in Arabidopsis protoplasts. Methods Mol Biol 774:59–71. https://doi.org/10.1007/978-1-61779-234-2_4

Lee MH, Hwang I (2014) Adaptor proteins in protein trafficking between endomembrane compartments in plants. J Plant Biol 57:265–273. https://doi.org/10.1007/s12374-014-0314-8

Lee J, Lee H, Kim J et al (2011a) Both the hydrophobicity and a positively charged region flanking the C-terminal region of the transmembrane domain of signal-anchored proteins play critical roles in determining their targeting specificity to the endoplasmic reticulum or endosymbiotic org. Plant cell 23:1588–1607. https://doi.org/10.1105/tpc.110.082230

Lee MH, Jung C, Lee J et al (2011b) An Arabidopsis prenylated Rab Acceptor 1 isoform, AtPRA1.B6, displays differential inhibitory effects on anterograde trafficking of proteins at the endoplasmic reticulum. Plant Physiol 157:645–658. https://doi.org/10.1104/pp.111.180810

Lee JM, Yang EC, Graf L et al (2018a) Analysis of the draft genome of the red seaweed *Gracilariopsis chorda* provides insights into genome size evolution in Rhodophyta. Mol Biol Evol 35:1869–1886. https://doi.org/10.1093/molbev/msy081

Lee DW, Yoo YJ, Razzak MA, Hwang I (2018b) Prolines in transit peptides are crucial for efficient preprotein translocation into chloroplasts. Plant physiol 176:663–677. https://doi.org/10.1104/pp.17.01553

Lindskog S (1997) Structure and mechanism of carbonic anhydrase. Pharmacol Ther 74:1–20. https://doi.org/10.1016/S0163-7258(96)00198-2

Liu S, Bugos RC, Dharmasiri N, Su WW (2000) Green fluorescent protein as a secretory reporter and a tool for process optimization in transgenic plant cell cultures. J Biotechnol 87:1–16

MacAuley SR, Zimmerman SA, Apolinario EE et al (2009) The archetype γ-class carbonic anhydrase (cam) contains iron when synthesized in vivo. Biochemistry 48:817–819. https://doi.org/10.1021/bi802246s

Marchler-Bauer A, Bo Y, Han L, He J, Lanczycki CJ, Lu S, Chitsaz F, Derbyshire MK, Geer RC, Gonzales NR, Gwadz M, Hurwitz DI, Lu F, Marchler GH, Song JS, Thanki N, Wang Z, Yamashita RA, Zhang D, Zheng C, Geer LY, Bryant SH (2016) CDD/SPARCLE: functional classification of proteins via subfamily domain architectures. Nucleic Acids Res 45:D200–D203. https://doi.org/10.1093/nar/gkw1129

Minh BQ, Nguyen MAT, Von Haeseler A (2013) Ultrafast approximation for phylogenetic bootstrap. Mol Biol Evol 30:1188–1195. https://doi.org/10.1093/molbev/mst024

Mitra M (2004) Identification of a new chloroplast carbonic anhydrase in *Chlamydomonas reinhardtii*. Plant Physiol 135:173–182. https://doi.org/10.1104/pp.103.037283

Moroney JV, Bartlett SG, Samuelsson G (2001) Carbonic anhydrases in plants and algae: invited review. Plant Cell Environ 24:141–153. https://doi.org/10.1046/j.1365-3040.2001.00669.x

Moroney JV, Ma Y, Frey WD et al (2011) The carbonic anhydrase isoforms of *Chlamydomonas reinhardtii*: intracellular location, expression, and physiological roles. Photosynth Res 109:133–149. https://doi.org/10.1007/s11120-011-9635-3

Nguyen LT, Schmidt HA, Von Haeseler A, Minh BQ (2015) IQ-TREE: A fast and effective stochastic algorithm for estimating maximum-likelihood phylogenies. Mol Biol Evol 32:174–268. https://doi.org/10.1093/molbev/msu300

Parisi G, Perales M, Fornasari MS et al (2004) Gamma carbonic anhydrases in plant mitochondria. Plant Mol Biol 55:193–207. https://doi.org/10.1007/s11103-004-0149-7

Park Y, Xu Z-Y, Kim SY et al (2016) Spatial regulation of ABCG25, an ABA exporter, is an important component of the mechanism controlling cellular ABA levels. Plant Cell 28:2528–2544. https://doi.org/10.1105/tpc.16.00359

Patro R, Duggal G, Love MI, Irizarry RA, Kingsford C (2017) Salmon provides fast and bias-aware quantification of transcript expression. Nat Methods 14:417–419. https://doi.org/10.1038/nmeth.4197

Razzak MA, Lee DW, Yoo YJ, Hwang I (2017) Evolution of rubisco complex small subunit transit peptides from algae to plants. Sci Rep 7:1–11. https://doi.org/10.1038/s41598-017-09473-x

Smith KS, Ferry JG (2000) Prokaryotic carbonic anhydrases. FEMS Microbiol Rev 24:335–366. https://doi.org/10.1016/S0168-6445(00)00030-9

Sohn EJ (2003) Rha1, an Arabidopsis Rab5 homolog, plays a critical role in the vacuolar trafficking of soluble cargo proteins. Plant Cell 15:1057–1070. https://doi.org/10.1105/tpc.009779

Supuran CT (2013) Carbonic anhydrases. Bio Med Chem 21:1377–1378. https://doi.org/10.1016/j.bmc.2013.02.026

Supuran CT, Capasso C (2017) An overview of the bacterial carbonic anhydrases. Metabolites. https://doi.org/10.3390/metabo7040056

Takeuchi M, Ueda T, Sato K et al (2000) A dominant negative mutant of Sar1 GTPase inhibits protein transport from the endoplasmic reticulum to the Golgi apparatus in tobacco and Arabidopsis cultured cells. Plant J 23:517–525. https://doi.org/10.1046/j.1365-313X.2000.00823.x

Villarejo A, Burén S, Larsson S et al (2005) Evidence for a protein transported through the secretory pathway en route to the higher plant chloroplast. Nat Cell Biol 7:1124–1131. https://doi.org/10.1038/ncb1330

Wang Q, Fristedt R, Yu X et al (2012) The γ-carbonic anhydrase subcomplex of mitochondrial complex I is essential for development and important for photomorphogenesis of Arabidopsis. Plant physiol 160:1373–1383. https://doi.org/10.1104/pp.112.204339

Wyszynski FJ, Hesketh AR, Bibb MJ, Davis BG (2010) Dissecting tunicamycin biosynthesis by genome mining: cloning and heterologous expression of a minimal gene cluster. Chem Sci 1:581. https://doi.org/10.1039/c0sc00325e

Xiang L, Etxeberria E, Van Den Ende W (2013) Vacuolar protein sorting mechanisms in plants. FEBS J 280:979–993. https://doi.org/10.1111/febs.12092

Ynalvez R, Xiao Y, Ward AS et al (2008) Identification and characterization of two closely related beta-carbonic anhydrases from *Chlamydomonas reinhardtii*. Physiol plant 133:15–26. https://doi.org/10.1111/j.1399-3054.2007.01043.x

Zimmerman SA, Ferry JG (2008) The beta and gamma classes of carbonic anhydrase. Curr Pharm Des 14:716–721

Zimmerman SA, Tomb JF, Ferry JG (2010) Characterization of CamH from *Methanosarcina thermophila*, founding member of a subclass of the γ class of carbonic anhydrases. J Bacteriol 192:1353–1360. https://doi.org/10.1128/JB.01164-09